Biomaterials 35 (2014) 5908–5920

Contents lists available at ScienceDirect

Biomaterials

journal homepage: www.elsevier.com/locate/biomaterials

The impact of a chlorotoxin-modified liposome system on receptor MMP-2 and the receptor-associated protein ClC-3

Chao Qin [a,b], Bing He [a], Wenbing Dai [a], Zhiqiang Lin [a], Hua Zhang [a], Xueqing Wang [a], Jiancheng Wang [a], Xuan Zhang [a], Guangji Wang [b,**], Lifang Yin [a,b,***], Qiang Zhang [a,*]

[a] State Key Laboratory of Natural and Biomimetic Drugs, School of Pharmaceutical Sciences, Peking University, Xueyuan Road, Beijing 100191, China
[b] Key Laboratory of Drug Metabolism and Pharmacokinetics, School of Pharmacy, China Pharmaceutical University, Tongjia Xiang, Nanjing 210009, Jiangsu, China

ARTICLE INFO

Article history:
Received 3 March 2014
Accepted 27 March 2014
Available online 16 April 2014

Keywords:
Chlorotoxin
Targeting drug delivery system
MMP-2
ClC-3
Receptor-associated protein

ABSTRACT

Currently, it is unknown whether a receptor-associated protein will be affected when a ligand modified delivery system interacts with its receptor. Besides, chlorotoxin (ClTx)-modified liposomes can target to glioma cells, but the target molecule is not clear: MMP-2, ClC-3 or both? Here a comparative study of ClTx-conjugated liposomes was conducted on two types of tumor cells: U87, a human glioma cell line with high expression of both MMP-2 and ClC-3, and A549, a human lung cancer cell line with expression of only MMP-2. ClTx-modified liposomes behaved similarly in these two cancer cells in terms of *in vitro* cell uptake, endocytosis pathway, intracellular trafficking and *in vivo* targeting efficacy, though the two tested cell lines were very different in ClC-3 expression. These results revealed that the targeted delivery of ClTx modified liposomes to U87 tumor was MMP-2-mediated and not correlated with the chloride channel ClC-3. On the other hand, ClTx modified on the liposomes did activate the receptor-associated protein ClC-3 via the binding with MMP-2, leading to the inhibition on cell migration and chloride currents. This is significant because cell migration is a key step in tumor metastasis. Interestingly, higher *in vitro* cellular uptake and lower *in vivo* tumor accumulation of liposomal systems was found in U87 compared to the A549 model, possibly due to the biological differences between *in vitro* and *in vivo* models. In general, ClTx-modified delivery systems may potentially target to tumors other than glioma that express a high level of MMP-2, and its effect on ClC-3 may help prevent tumor metastasis.

1. Introduction

Cellular membranes consist of lipid and various types of membrane proteins, including receptors and ion channels located in special membrane domains. It is estimated that approximately 30% of human genome encodes membrane proteins [1,2]. These membrane proteins may play important roles in cell signaling cascades, membrane fusion, cell to cell communication, ion transport, cell adhesion, cell volume regulation, and even drug discovery, because the targets for over 70% of therapeutic drugs are membrane proteins [3,4]. On the other hand, the active targeting system is usually established by modification with antibodies, antibody fragments or peptides generally called ligands [5]. With ligands interacting with receptors over-expressed on the surface of tumor cells, the active targeting nanomedicines increase the cellular uptake of drugs into cancer cells on the basis of the EPR effect *in vivo* [6,7]. Many active targeting systems present satisfying specificity, and some of them are now in advanced phases of clinical trials [8]. Because some membrane proteins are closely localized together, such as receptors and receptor-associated proteins, when one such protein is activated, the function of other associated protein is probably affected. However, most previous studies on active targeting only focus on the interaction between the ligands and receptors. It is currently unclear whether the receptor-associated proteins will also be affected when the ligands modified on the nanomedicines interacts with receptors on the cells.

* Corresponding author. State Key Laboratory of Natural and Biomimetic Drugs, School of Pharmaceutical Sciences, Peking University, Xueyuan Road, Beijing 100191, China. Tel./fax: +86 10 82802791.
** Corresponding author. Key Laboratory of Drug Metabolism and Pharmacokinetics, School of Pharmacy, China Pharmaceutical University, Tongjia Xiang, Nanjing 210009, Jiangsu, China. Tel./fax: +86 25 83271128.
*** Corresponding author. Key Laboratory of Drug Metabolism and Pharmacokinetics, School of Pharmacy, China Pharmaceutical University, Tongjia Xiang, Nanjing 210009, Jiangsu, China. Tel./fax: +86 25 86185258.
E-mail addresses: guangjiwang@hotmail.com (G. Wang), lifangyin@hotmail.com (L. Yin), zqdodo@bjmu.edu.cn (Q. Zhang).

http://dx.doi.org/10.1016/j.biomaterials.2014.03.077
0142-9612/

Chlorotoxin (ClTx) purified from the venom of the scorpion *Leiurus quinquestriatus* is a peptide containing 36 amino acids and 4 disulfide bonds at a relative molecular mass of 3996 [9]. A membrane protein, matrix metalloproteinase-2 (MMP-2) has been shown to be the receptor for ClTx [10]. Additionally, it has been found that ClTx could inhibit a voltage gated chloride channel specifically expressed on human astrocytoma and glioma cells as well as acute slices of human gliomas [11,12]. This chloride channel was then identified as ClC-3, a type of Cl^- / H^+ exchanger mainly expressed in endosomal/lysosomal compartments (>95%), and nowadays, ClTx is still considered as the only specific inhibitor of ClC-3 [13–15]. Interestingly, it was supposed that ClC-3 and MMP-2 formed a protein complex located in the same membrane domain, and the interaction of ClTx with MMP-2 decreased the surface expression of ClC-3 and obstructed the chloride currents [16], revealing the effects of ClTx on both receptor MMP-2 and the receptor-associated protein ClC-3.

After the selective binding of ClTx to glioma cells and other tumors of neuroectodermal origin was verified, a few reports utilized ClTx as the targeting ligand to deliver drug, gene or diagnosis agent [9,17–21]. However, the target molecule of ClTx-modified nanomedicines is still unknown: MMP-2, ClC-3 or both membrane proteins, though the chloride channel was supposed as the delivery target in our previous study [21]. Further, the impact of any interactions and the relationship between MMP-2 and ClC-3 during the targeted delivery are also unclear currently, except the supposition that they formed a protein complex in a special membrane domain [16].

To address these issues, a comparative study of chlorotoxin-conjugated liposomes on both MMP-2 and the associated protein ClC-3 in two types of tumor cells was conducted here. ClTx modified liposomes were fabricated and characterized as a model of a receptor-mediated delivery system. U87 MG (U87), a human glioblastoma cell line with high expression of both MMP-2 and ClC-3, was selected as the experimental cell model, while A549, a human lung cancer cell line with high expression of only MMP-2, was used as the control cell model. The co-localization between MMP-2 and ClC-3 in U87 cells was confirmed. Then, the *in vitro* cellular uptake, endocytosis pathway, intracellular trafficking and *in vivo* near-infrared imaging of ClTx modified liposomes, as well as the inhibition effect on migration and chloride currents by this modified system, were compared in these two cell types.

2. Materials

N-hydroxysuccinimidyl-PEG_{2000}-DSPE and DSPE-PEG_{2000} were purchased from NOF Corporation (Tokyo, Japan). ClTx was synthesized by ChinaPeptides Co., Ltd (Shanghai, China). Hydrogenated soybean phospholipids (HSPC) was purchased from Lipoid GmbH (Ludwigshafen, Germany). Cholesterol, Sephadex G-50, trichloroacetic acid (TCA), sulforhodamine B (SRB), anhydrous N, N-dimethylformamide (DMF), chlorpromazine, filipin, methyl-beta-cyclodextrin (MβCD) and 5-(N-ethyl-N-isopropyl)-amiloride (EIPA) were purchased from Sigma–Aldrich (St. Louis, MO, USA). Tris was purchased from Amresco (Solon, OH, USA). Doxorubicin Hydrochloride (Dox) was kindly presented by Hisun Pharm (Zhejiang, China). Dir, Hoechst 33258, Coumarin-6 (C6), LysoTracker Red and 6-methoxy-N-ethylquinolinium iodide (MEQ) were purchased from Life Technologies (Eugene, USA). Cell counting kit-8 (CCK-8) was purchased from Dojido Laboratories (Tokyo, Japan). Rabbit polyclonal to CIC-3 and mouse monoclonal to MMP-2 were purchased from Abcam (Cambridge, UK). Secondary antibodies labeled with Texas red or FITC were from Proteintech (Chicago, USA). ER-Tracker Red was purchased from Beyotime (Jiangsu, China). Other reagents were all of ACS grade or HPLC grade.

2.1. Cell culture and animals

The human glioblastoma cell line U87 MG (U87) and human lung carcinoma cell line A549 were obtained from Cell Resource Center, Institute of Basic Medical Sciences, Chinese Academy of Medical Sciences (Beijing, China). U87 cells were cultured in MEM medium containing a final concentration of 10% (v/v) fetal bovine serum (FBS), 1% nonessential amino acid and 1% antibiotics (penicillin, 100 U/mL plus streptomycin). A549 cells were cultured in F12K medium plus 10% FBS and 1% antibiotics. Both cell lines were cultured at 37 °C in humidified atmosphere with 5% CO_2.

Female BALB/c nude mice of 6–8 weeks old were from Vital River Company (Beijing, China) and kept under SPF condition with free access to standard food and water during the experiment. All experiments of animals were performed under the guidelines of the Ethics Committee of Peking University.

2.2. Synthesis of DSPE-PEG-ClTx and preparation of liposomes

The synthesis method of targeting material DSPE-PEG-ClTx and preparation of liposomes were previously reported by our research group [21]. In brief, DSPE-PEG-NHS and ClTx (5:1; molar ratio) were reacting for 120 h in DMF adjusted to pH 8 with triethylamine. The conjugation efficiency was monitored by reverse high performance liquid chromatography (HPLC). After dialysis and freeze-drying, the targeting material was confirmed by matrix-assisted laser desorption/ionization time of flight mass spectrometry (MALDI-TOF; Bruker Daltonics, USA).

The Dox-loading liposomes modified with ClTx (ClTx-SSL-Dox) and non-modified liposomes loading Dox (SSL-Dox) were prepared by thin film hydration followed by the ammonium sulfate transmembrane gradient method [21]. The liposomes loaded with C6 or DiR (ClTx-SSL-C6, SSL-C6 or ClTx-SSL-DiR, SSL-DiR) were directly prepared by thin film hydration.

2.3. Expression and localization of ClC-3 and MMP-2

2.3.1. Receptor expression of MMP-2 and ClC-3 in U87 and A549 cell lines

U87 or A549 cells were cultured on 12 mm glass cover slips for 24 h at 37 °C. The cells were washed twice with PBS and fixed with 4% paraformaldehyde for 20 min. When the fixative was removed, the cells were washed three times with PBS and then immersed in blocking buffer (5% BSA in PBS) for 1 h. The cells were incubated overnight at 4 °C with primary antibodies against ClC-3 or MMP-2, respectively, diluted in blocking buffer. Then, the cells were washed three times with PBS, and incubated at 37 °C for 1 h with Texas red-labeled goat anti-rabbit or FITC-labeled goat anti-mouse secondary antibodies, respectively. Finally, the nuclei were stained with Hoechst 33258 for 15 min, and the fluorescent signal was imaged with a laser scanning confocal microscope (Leica, Heidelberg, Germany).

2.3.2. Co-localization of ClC-3 and MMP-2 in U87 cells

For immunofluorescence of ClC-3 and MMP-2 in U87 cells, after fixation with 4% paraformaldehyde and blocked with 5% BSA, the cells were incubated in the primary antibodies mixture diluted with blocking solution at 4 °C overnight. Then the cells were stained with dye-labeled secondary antibodies, and the nuclei were stained with Hoechst 33258. The co-localization of ClC-3 and MMP-2 was observed with confocal microscopy (Leica, Heidelberg, Germany).

2.4. Demonstration of MMP-2 mediated targeting delivery for ClTx-modified liposomes

2.4.1. In vitro cellular uptake

U87 or A549 cells were seeded in 12-well cell culture clusters (Corning, NY, USA) at a density of 3×10^5 cells per well. On the following day, the confluent cells were incubated with Dox loaded liposomes including SSL-Dox and ClTx-SSL-Dox (containing Dox at 30 μg/mL) in serum-free medium at 37 °C in darkness for 3 h. Meanwhile, the cells treated with medium were used as negative control. After incubated, the cells were washed 3 times with cold PBS, trypsinized, harvested and washed 3 times by centrifugation and resuspension in PBS. The mean fluorescence intensity of Dox in cells was measured with a FACScan flow cytometer (Becton Dickinson FACS Calibur, USA).

For confocal imaging, cells seeded on a 12-mm round glass cover slips were treated with SSL-Dox and ClTx-SSL-Dox (containing Dox 30 μg/mL) at 37 °C for 3 h. Then, the cells were washed three times with cold PBS and fixed with 4% paraformaldehyde for 15 min. After nucleus staining with Hoechst 33258, the fluorescent signal was imaged with a laser scanning confocal microscope (Leica, Heidelberg, Germany).

2.4.2. Competitive inhibition assay

Antibody competitive inhibition assay was used to confirm the receptor of the ClTx modified liposomes. The U87 or A549 cells were pre-treated with antibody to ClC-3 and antibody to MMP-2 for 1 h, respectively, followed by incubation with modified liposomes in serum-free medium containing the antibody, and the cells incubated with non-modified liposomes or modified liposomes without antibody pre-treatment were the control group. Then, the cellar uptake of liposomes was measured with a FACScan flow cytometer (Becton Dickinson FACS Calibur, USA).

2.4.3. Cytotoxicity assay

Cytotoxicity of different Dox loaded liposomes against U87 or A548 cells was evaluated to further investigate the ClTx modification effect. U87 or A549 cells were cultured in 96 well cell culture plate at a density of 5×10^3 cells per well for 24 h. Then, the cells were treated with serial concentration of SSL-Dox, and ClTx-SSL-Dox,

respectively. After 48 h, the drug-containing medium was removed by aspiration and each well was washed twice with PBS. The SRB assay was utilized to evaluate the cytotoxicity of different liposomes [22]. In brief, after fixation with 10% TCA and air dried, the fixed cells were stained with 0.4% SRB at room temperature for 30 min and washed with 1% acetic acid. After the dye was dissolved in 10 mM Tris base solution, the absorbance of each well was measured in a Multiscan FC microplate reader (ThermoFisher scientific, MA, USA) at the wavelength of 540 nm. The survival rates of cells were calculated.

2.5. Intracellular fate investigation of ClTx-modified liposomes

2.5.1. Endocytosis pathway detection by uptake inhibitors

The U87 or A549 cells were pre-treated with different inhibitors for 1 h, the kinds of inhibiters and their concentrations were as follows: chlorpromazine, 30 μM; filipin, 15 μM; MβCD, 10 mM, EIPA, 20 μM. Next, the inhibitors were removed, and the cells were incubated with modified liposomes for 3 h. Then, the cellar uptake of liposomes was measured by flow cytometry (Becton Dickinson FACS Calibur, USA).

Cytotoxicities of inhibitors on U87 and A549 cells were evaluated with the CCK-8 cytotoxicity assay. Briefly, cells seeded in 96 well cell culture plate at a density of 5×10^3 cells per well were incubated with different inhibitors for 1 h using the concentrations mentioned above, with cells incubated with FBS-free medium as control. Then the medium containing inhibitors was removed and the cells were treated with new FBS free medium followed by the addition of CCK-8 solution. After 2 h, the Multiscan FC microplate reader (ThermoFisher scientific, MA, USA) was used to record the absorbance at 450 nm and the survival rates of cells were calculated.

2.5.2. Intracellular trafficking

A549 or U87 cells was seeded on 12-mm round glass cover slips and cultured for 24 h. The medium was removed, and the cells were incubated with medium containing LysoTracker Red (100 nM) for 2 h at 37 °C. Then the cells were treated with liposomes loading C6 for 20 min or 60 min. Then the cells were washed with PBS and nuclei were stained with Hoechst 33258 following fixation. The samples were imaged with a laser scanning confocal microscope and the co-localization correlation and the co-localization rate were determined by software associated with the confocal microscope (Leica, Heidelberg, Germany).

In the endoplasmic reticulum co-localization experiment, cells cultured for 24 h were incubated with ER-Tracker Red (1 μM) for 30 min. The rest of the operation procedure was the same as for the co-localization with lysosomes.

2.6. In vivo targeting efficiency

The BALB/c nude mice bearing two types of tumors were prepared. In detail, 1×10^7 U87 cells suspended in 100 μL culture medium without FBS were injected into right subcutaneous dorsa of mice, and 1×10^7 A549 cells were injected into the left subcutaneous dorsa. After 3 weeks, 200 μL of DiR-loading liposomes were intravenously injected through the tail vein into mice bearing tumors at a dose of 40 μg/kg. Mice were anaesthetized with isoflurane and the distribution of liposomes was imaged with an *in vivo* imaging system (Carestream Molecular Imaging, New Haven, USA) at predetermined time intervals. After the final time point, the mice were sacrificed, and the tumors and the major organs were excised for *ex vivo* imaging.

2.7. The effect on ClC-3 of ClTx modified liposomes

2.7.1. Migration assay

The transwell migration assay was used to evaluate the migration inhibition of free ClTx, liposomes and modified liposomes. The inserts with polycarbonate membranes containing 8 μm pores were washed with PBS, and incubated in 1% bovine serum albumin (BSA) for 1 h. Then, the inserts were kept in serum-free culture medium with 0.1 BSA until cell seeding. U87 and A549 cells were harvested and suspended in FBS-free culture medium at a concentration of 4×10^5/mL, and 100 μl cell suspensions was plated on the upper surface of the insert. The inserts were kept in 24-well culture plates, and medium containing 10% FBS were added outside the inserts as attractant. The free ClTx and ClTx modified liposomes were added to make the final concentration of ClTx at 1 μM. An equal volume of non-modified liposomes or PBS was added as a compared group and a negative

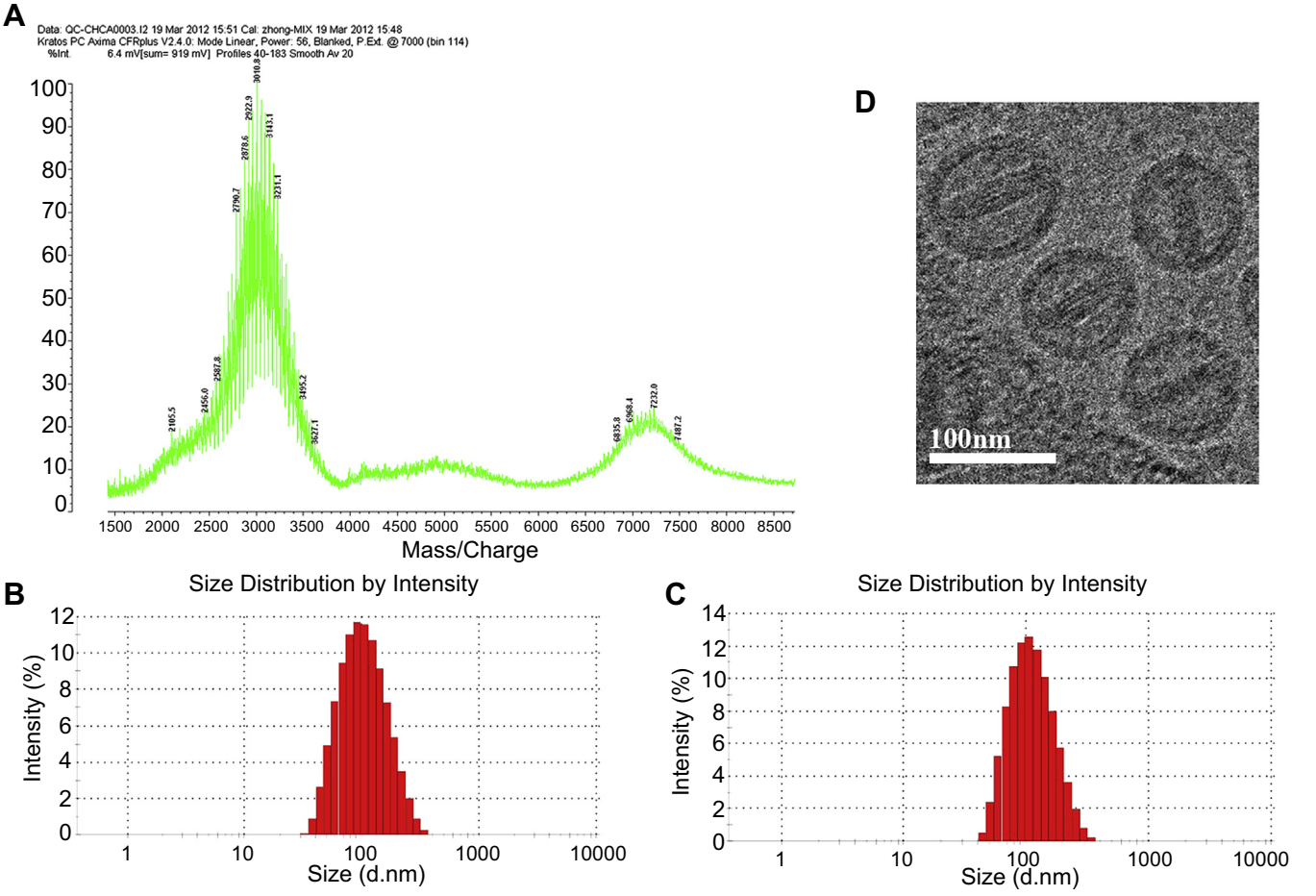

Fig. 1. Characterization of the targeting material and the liposomes. A: MALDI-TOF results of the targeting material. B–C: Particle size distribution of SSL-Dox (average size, $d = 95.67$ nm) and ClTx-SSL-Dox (average size, $d = 103.14$ nm) by intensity. D: Cryo-TEM image of ClTx-SSL-Dox.

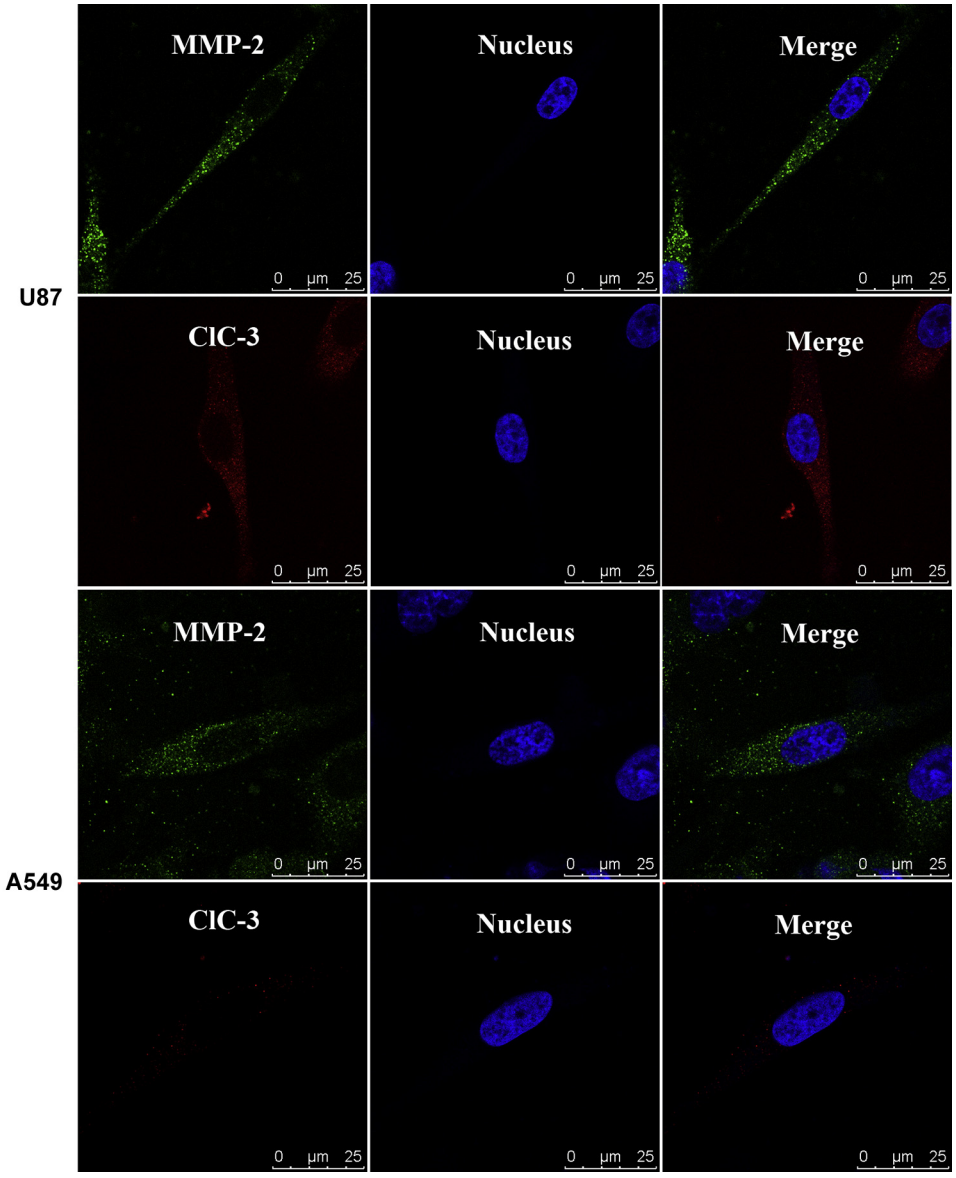

Fig. 2. Receptor expression of MMP-2 and ClC-3 in U87 and A549 cells with the method of immunofluorescence.

control group. The transwell plates were returned to the humidified incubator at 37 °C. After 24 h, the inserts were washed with PBS, and the cells on the upper surface of inserts were scrubbed off with humid cotton buds, while the cells on the bottom surface were fixed with methanol for 20 min and stained with 0.1% crystal violet solution for 30 min. Nine visual fields of cells on the bottom of each insert were counted with an optical microscope (Nikon, Kanagawa, Japan), and the inhibition rate was calculated compared with blank control groups.

2.7.2. Measurement of chloride currents by MEQ

The chloride-sensitive dye 6-methoxy-N-ethylquinolinium iodide (MEQ) was prepared as protocol of the manufacturer. Briefly, 1 mg of MEQ was dissolved in 20 μl of distilled water in a glass test tube and then the MEQ was reduced with 20 μl of 12% aqueous solution of sodium borohydride under continual flow of nitrogen gas for 30 min. Then, the 6-methoxy-N-ethyl-1, 2-dihydroquinoline (DiH-MEQ) was extracted from the reaction mixture with ethyl ether. After the ethyl ether was evaporated, 50 μM of DiH-MEQ as a loading solution was prepared by dissolving the yellow oil directly into an isotonic solution without Cl^-, containing (in mM): sodium gluconate 130, potassium gluconate 5.4, calcium gluconate 1.2, magnesium sulfate 0.8, sodium dihydrogen phosphate 1, glucose 5.5 and Tris 5. The cells cultured in 96-well cell plates at a density of 2×10^4 cells per well for 24 h were incubated with the loading solution for 10 min at 37 °C in dark, and then the cells were washed and incubated with Cl^--free solution for 10 min to uniform the distribution of the dye in the cytoplasm. The fluorescence intensity of the dye was measured every 2 min using a fluorescence plate reader (Molecular Devices, CA, USA) with 340 nm excitation and 440 emission filters. During the measurement, the isotonic solution was replaced with hypotonic solution containing (in mM): sodium gluconate 80, potassium gluconate 5.4, calcium gluconate 1.2, magnesium sulfate 0.8, sodium dihydrogen phosphate 1, glucose 5.5, sodium chloride 30 and Tris 5. As the test groups, the cells were pre-incubated with free ClTx (1 μM), blank liposomes or ClTx-modified blank liposomes for 1 h.

2.8. Statistical analysis

All of the experiments were repeated at least three times. Data are shown as the means ± standard deviation (SD). Student's *t*-test was used to identify significant differences. *P* values less than 0.05 were considered statistically significant.

3. Results and discussions

3.1. Synthesis of DSPE-PEG-ClTx and preparation of liposomes

The MALDI-TOF profile of the targeting material is shown in Fig. 1A. In detail, the peak of 3996 (the original Mw of ClTx) was almost absent while the peak of 7000 Mw (DSPE-PEG-ClTx) was clear, indicating the synthesis of targeting material with high

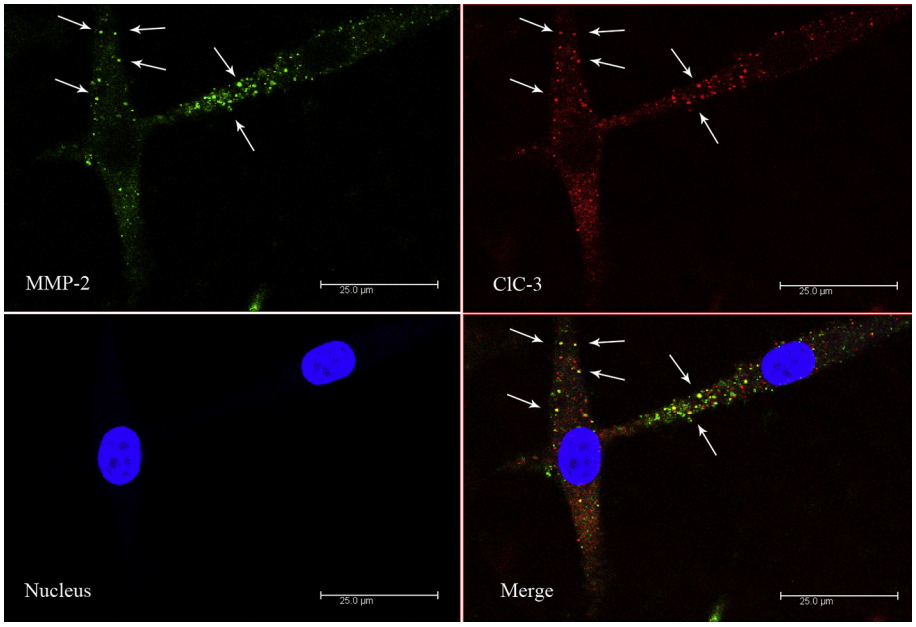

Fig. 3. Co-localization of MMP-2 and ClC-3 on U87 cells with the method of immunofluorescence. (The arrows indicate parts of the co-localization sites).

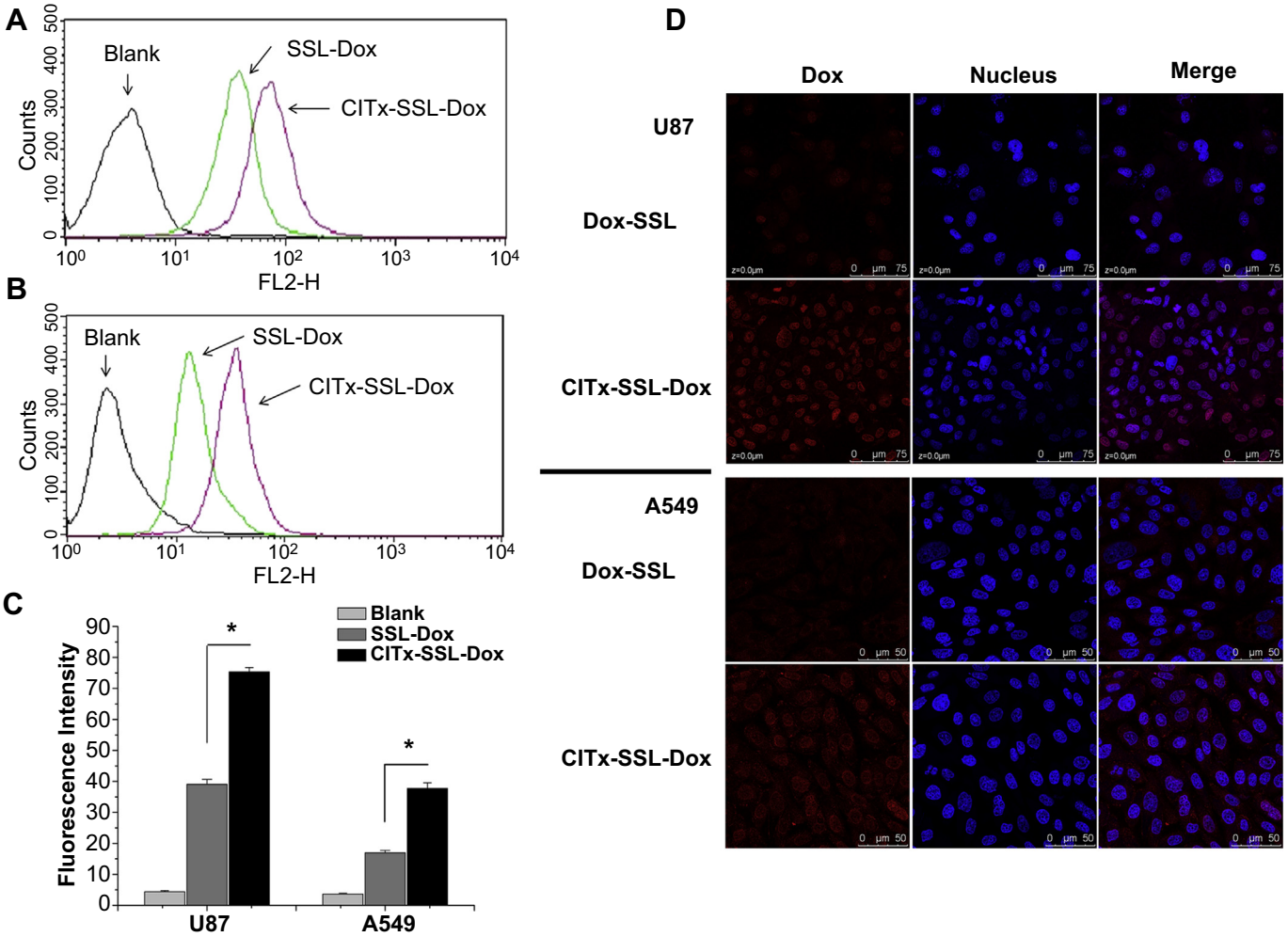

Fig. 4. The cellular uptake of SSL-Dox and CITx-SSL-Dox in U87 and A549 cells. A, B: Flow cytometry analysis of the U87 (A) and A549 cells (B) treated with SSL-Dox and CITx-SSL-Dox for 3 h at 37 °C using a Dox-free medium as control. C: Quantitative results of flow cytometry analysis. D: Laser scanning confocal microscopy images of the U87 and A549 cells incubated with SSL-Dox and CITx-SSL-Dox.

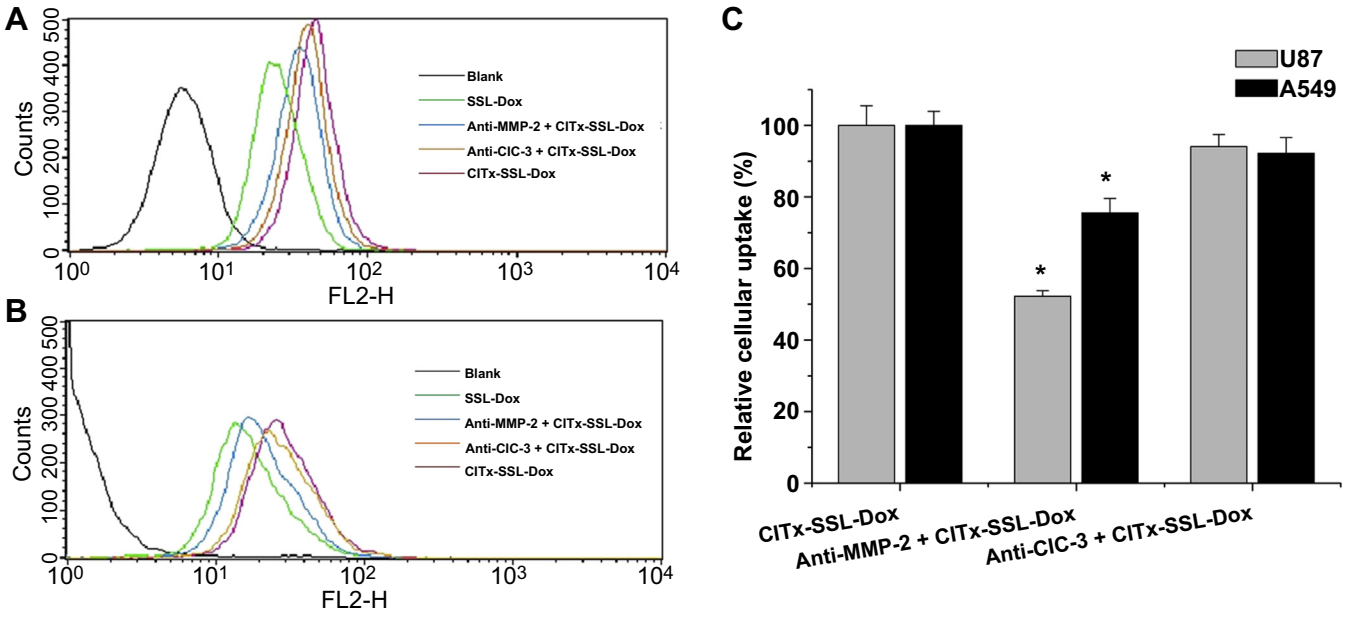

Fig. 5. Competitive inhibition of the cellular uptake of CITx-SSL-Dox. Prior to the addition of SSL-Dox and CITx-SSL-Dox, the cells were incubated with the antibody against MMP-2 or ClC-3 for 1 h. A, B: Competitive inhibition effect with flow cytometry analysis in U87 (A) and A549 cells (B). C: Quantitative results of flow cytometry analysis. (*$p < 0.05$, significant difference between the CITx-SSL-Dox group and the antibody treated group in U87 or A549, respectively.)

conjugation efficiency (>95% confirmed by HPLC assay). The dynamic light scattering analysis with a Malvern Zetasizer Nano ZS (Malvern; Worcestershire, UK) and morphological observation with a cryogenic transmission electron microscopy (cryo-TEM; Philips, Netherlands) revealed that the particle size of the CITx modified liposomes was about 100 nm, and the CITx modification did not affect their size significantly (Fig. 1B–D).

3.2. Expression and localization of ClC-3 and MMP-2

3.2.1. Receptor expression of MMP-2 and ClC-3 in U87 and A549 cell lines

ClC-3 and MMP-2 expression levels in U87 or A549 cells are shown in Fig. 2. MMP-2 was expressed in both the U87 and A549 cells at similar levels. Meanwhile, the U87 cells expressed a significantly higher level of ClC-3 than A549 cells, which barely expressed ClC-3. MMP-2 is a type of secreted MMPs and ClC-3 was also expressed on the surface of intracellular vesicles and endosomes [23–25]. So in the Fig. 2, it is worth noting that MMP-2 and ClC-3 receptors were not only expressed on the surface of the cells, but were present in the cytoplasm.

3.2.2. Co-localization of ClC-3 and MMP-2 in U87 cells

Further evaluations of the co-localization of ClC-3 and MMP-2 in U87 cells are illustrated in Fig. 3. Numerous yellow spots in merged images were observed (white arrows), exhibiting significant co-localization of ClC-3 and MMP-2. Interestingly, more obvious merged signals were found in the cell membrane than in the cytoplasm, indicating that more ClC-3 and MMP-2 on the cell membrane simultaneously co-localized in a membrane domain,

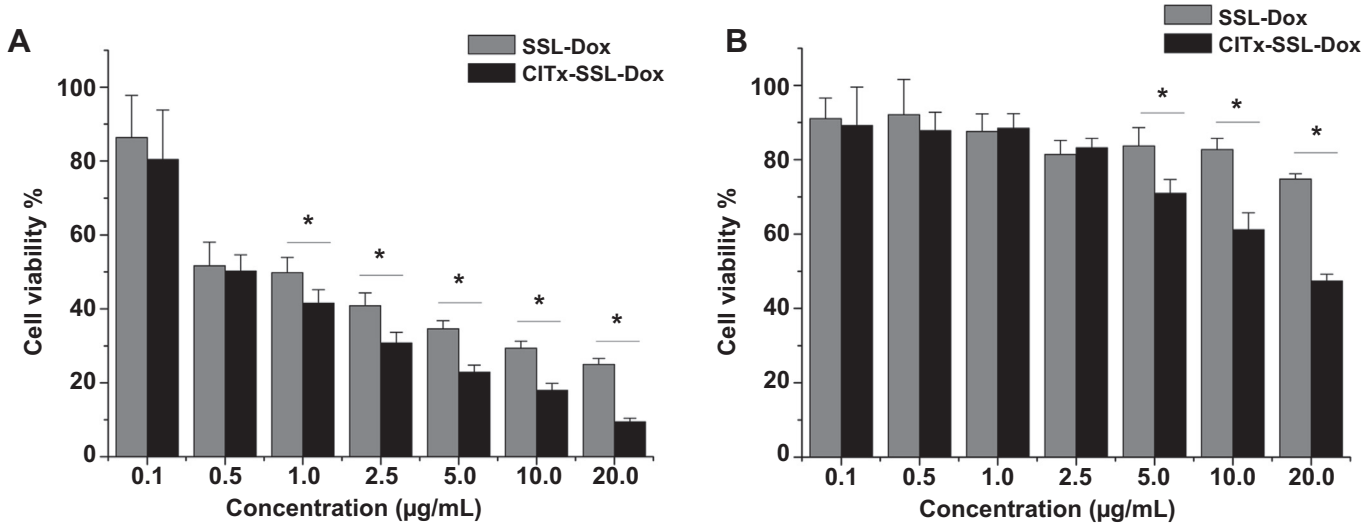

Fig. 6. Cytotoxicity of SSL-Dox and CITx-SSL-Dox against U87 (A) and A549 cells (B) at different concentration of Dox with SRB assay. The cells were treated with SSL-Dox or CITx-SSL-Dox for 48 h (*$p < 0.05$).

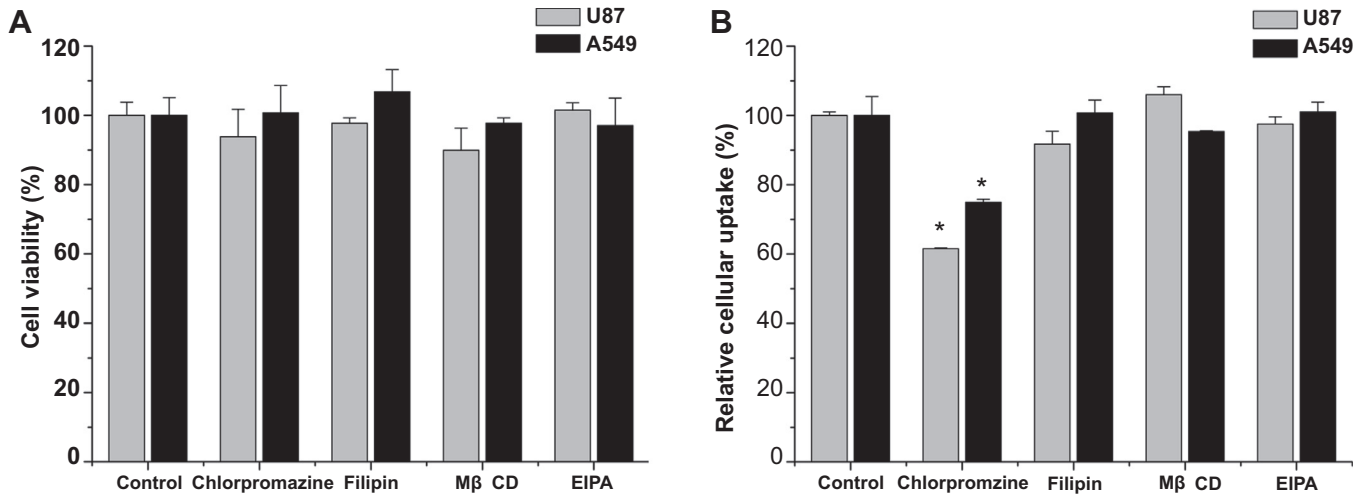

Fig. 7. Effects of inhibitors on the uptake of ClTx-SSL-Dox in U87 and A549 cells. A: CCK-8 assays of cell viability after incubation with inhibitors for 1 h. B: Prior to the treatment of ClTx-SSL-Dox, the cells were incubated with different inhibitor for 1 h ($^*p < 0.05$, significant difference between the ClTx-SSL-Dox group and the inhibitor treated group in U87 or A549 cells, respectively.)

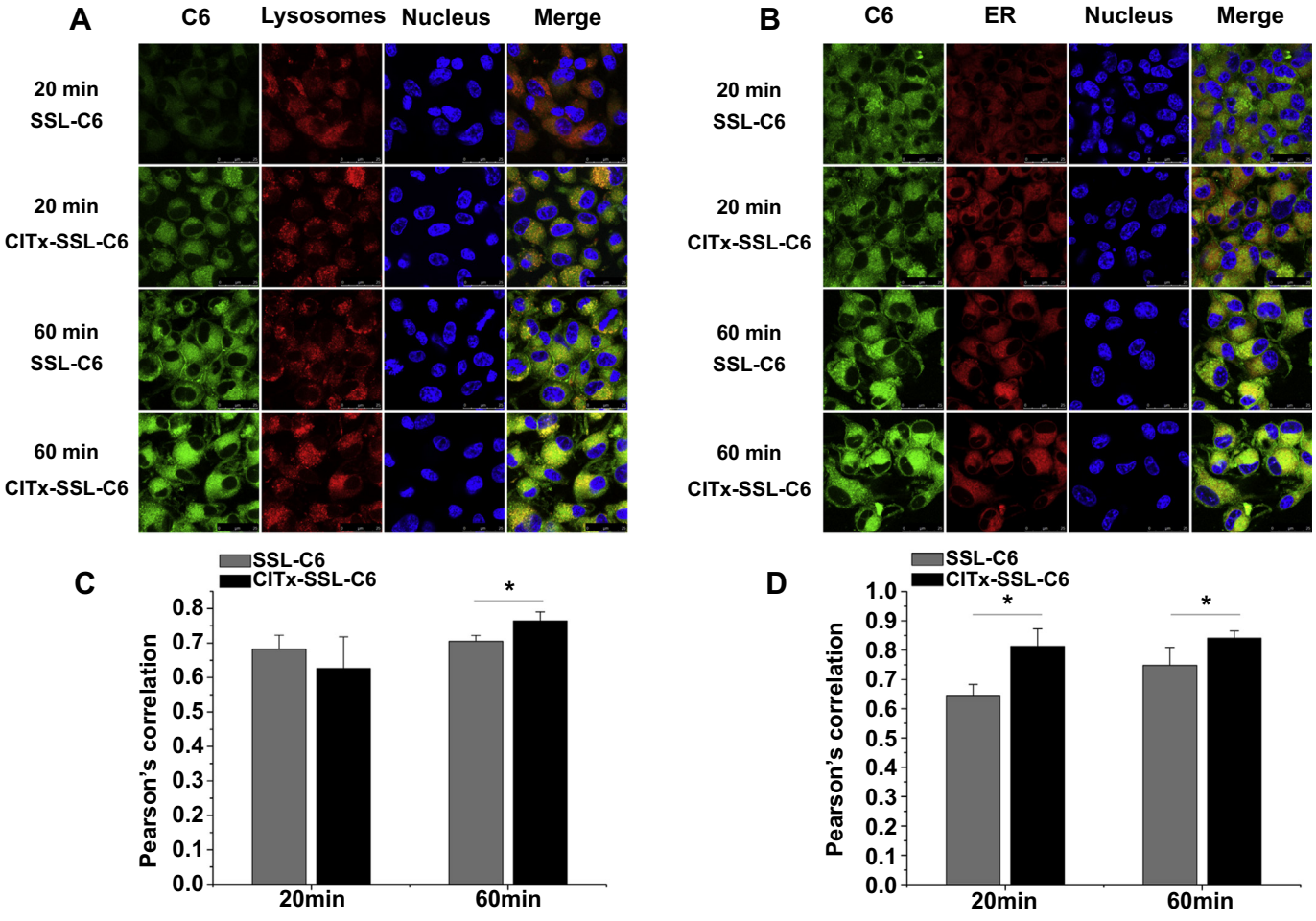

Fig. 8. Co-localization analysis of SSL-C6 or ClTx-SSL-C6 with lysosome and ER in U87 cells. A: Co-localization analysis of SSL-C6 or ClTx-SSL-C6 with lysosome at 20 min and 60 min. After treatment with Lyso-tracker (100 nM) for 2 h, the cells were incubated with SSL-C6 and ClTx-SSL-C6 (C6, 100 ng/mL) for 20 min or 60 min. B: Co-localization analysis of SSL-C6 or ClTx-SSL-C6 with ER at 20 min and 60 min. After treatment with ER-tracker (1 μM) for 0.5 h, the cells were incubated with SSL-C6 and ClTx-SSL-C6 (C6, 100 ng/mL) for 20 min or 60 min. C, D: Quantitative co-localization analysis of SSL-C6 and ClTx-SSL with lysosomes and ER. ($^*p < 0.05$).

consistent with previous reports [10,16]. Generally, we confirmed that ClC-3, as an associated protein, located next to MMP-2 in cell membrane.

3.3. MMP-2 mediated specificity of ClTx-modified liposomes in vitro

3.3.1. Endocytosis

The cellular uptake characteristics of ClTx modified liposomes in U87 and A549 cell lines monitored by flow cytometry are shown in Fig. 4A and B. DOX loaded here in two liposome systems was as used as a fluorescence marker. Notably, whether in U87 or A549 cells, the ClTx modification increased the cellular uptake of DOX. As shown in the statistical results in Fig. 4C, ClTx-modified liposomes exhibited significant endocytosis increases in endocytosis in comparison to non-modified liposomes, 2.1-fold in U87 cells and 2.5-fold in A549 cells. Further, it was noteworthy that the U87 cells had better uptake ability for both liposome systems than A549 cells, likely due to the difference in cell types. The confocal images in Fig. 4D further confirmed the data from flow cytometry, and the fluorescent intensity of cells treated with ClTx-modified liposomes was stronger than that of non-modified ones, especially in the nuclei.

Although there were differences in the expression level of ClC-3 protein between A549 and U87 cells, ClTx modification enhanced the cellular uptake of liposomes to a similar extent in both cell types, indicating that the targeting efficiency of ClTx-modified liposomes was not relevant with ClC-3. This revealed again that the receptor of ClTx was MMP-2 indeed [10], and that the expression level of MMP-2 in both cell lines was similar, as found above.

3.3.2. Competitive inhibition assay

Fig. 5 shows the uptake of ClTx-modified liposomes in U87 and A549 cells pre-treated with antibody to MMP-2 was lower than that in non-treated cells. However, the incubation of antibody to ClC-3 hardly affected the cellular uptake. These findings directly supported the conclusion that the ClTx conjugation improved the specific uptake of liposomes in both U87 and A549 cells via MMP-2 rather than ClC-3 mediation. Namely, MMP-2, but not ClC-3, was the targeting receptor that directly interacted with the ClTx modified on the surface of liposomes.

3.4. Cytotoxicity assay

As shown in Fig. 6, compared to non-modified liposomes, the ClTx modification exhibited higher cytotoxicity against U87 and A549 cells after 48 h incubation. Specifically, the targeting system showed significantly stronger effects for the concentration range of 5.0–20 μg/mL of Dox in A549 cells and for 1.0–20 μg/mL in U87 cells, when compared to non-targeting one. Further, at the same concentrations, both liposome formulations showed higher

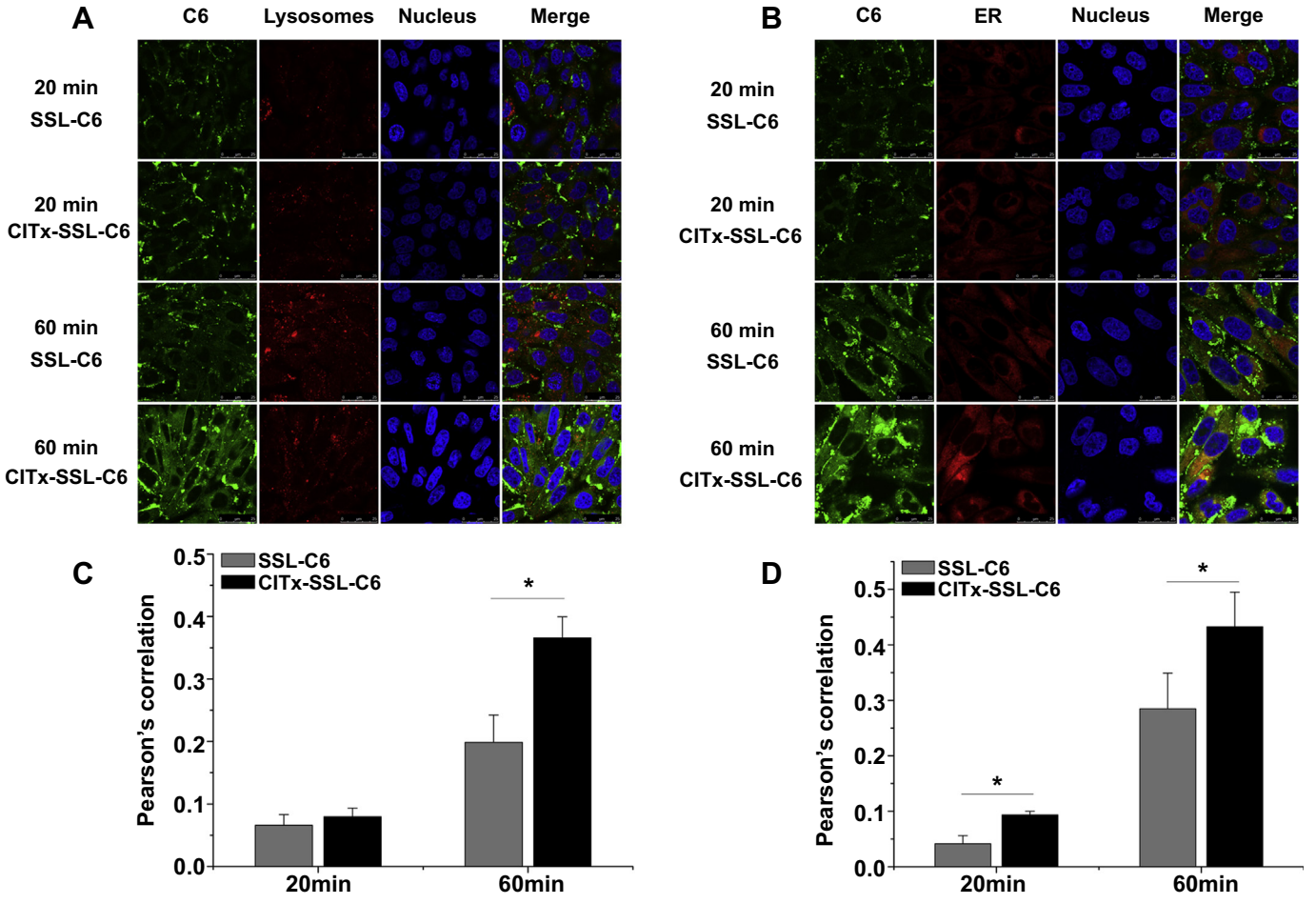

Fig. 9. Co-localization analysis of SSL-C6 or ClTx-SSL-C6 with lysosome and ER in A549 cells. A: Co-localization analysis of SSL-C6 or ClTx-SSL-C6 with lysosome at 20 min and 60 min. After treatment with Lyso-tracker (100 nM) for 2 h, the cells were incubated with SSL-C6 and ClTx-SSL-C6 (C6, 100 ng/mL) for 20 min or 60 min. B: Co-localization analysis of SSL-C6 or ClTx-SSL-C6 with ER at 20 min and 60 min. After treatment with ER-tracker (1 μM) for 0.5 h, the cells were incubated with SSL-C6 and ClTx-SSL-C6 (C6, 100 ng/mL) for 20 min or 60 min. C, D: Quantitative co-localization analysis of SSL-C6 and ClTx-SSL with lysosomes and ER. ($^*p < 0.05$).

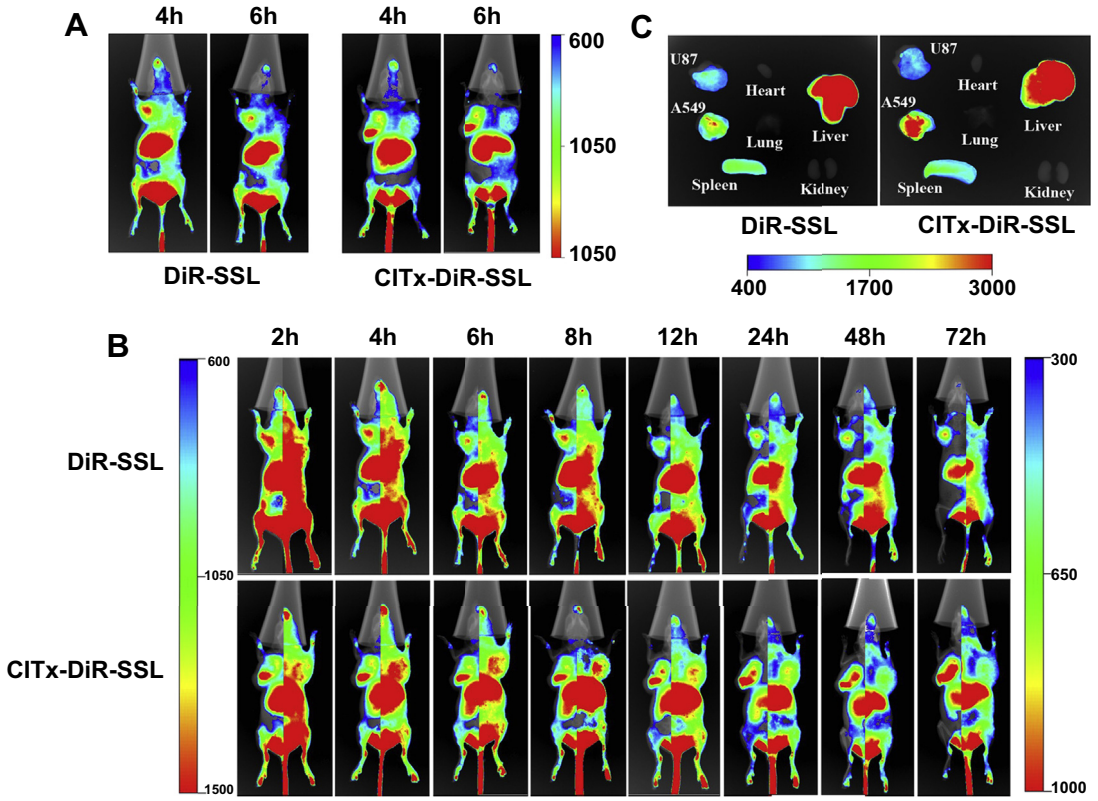

Fig. 10. *In vivo* targeting efficiency of SSL-DiR and ClTx-SSL-DiR in BALB/c nude mice bearing A549 and U87 tumors (DiR, 40 μg/kg). A: *In vivo* near-infrared fluorescence images of nude mice after intravenous administration of SSL-DiR or ClTx-SSL-DiR at 4 h and 6 h. B, C: One side *in vivo* near-infrared fluorescence images of nude mice after intravenous administration of the formulations at different time points (B, U87 tumor at right; C, A549 tumor at left). D: *Ex vivo* image of tumors and main organs after the double tumor-bearing nude mice were sacrificed at 72 h.

cytotoxicity in U87 than in A549 cells. This is probably because the uptake of liposomes by A549 cells was lower than that by U87 cells, as shown in Fig 4C, indicating the effect from the difference of cell lines. Generally, no matter in U87 or A549 cells, the ClTx modification increased the cytotoxicity, and this consistent with the cellular uptake.

3.5. Intracellular fate of ClTx modified liposomes

3.5.1. Endocytosis pathway of ClTx modified liposomes

The cellular endocytosis pathways of nanoparticles may differ depending on the modification of various targeting ligand and cell types such as cell origin, cell phenotype and so on [26,27]. Here, we investigated the endocytosis pathway of ClTx-modified liposomes in U87 and A549 cells by using different inhibitors (Fig. 7B). This evaluation was validated by preliminary experiments to confirm the cell viabilities higher than 80% with all inhibitors at the test concentrations (Fig. 7A). Chlorpromazine, an inhibitor of clathrin-mediated transport [28], induced a significant inhibitory effect on both U87 and A549 cells. Filipin and MβCD are inhibitors of caveolar dependent endocytosis through different mechanisms [29,30]. In this study, no obvious caveolar dependent endocytosis was found because both filipin and MβCD showed no inhibition effect on the cellular uptake. Another main endocytosis pathway, macropinocytosis, was investigated utilized EIPA, a derivative of amiloride blocking sodium-proton exchange [31]. Here, macropinocytosis was not involved in the endocytosis of modified liposomes in either cell line. Even in the chlorpromazine treated group, the inhibition rates were only 40.8% in U87 and 25.3% in A549, revealing the possible involvement of a clathrin/caveolar/macropinocytosis independent pathway in the endocytosis of modified liposomes [32].

In general, the cellular endocytosis of ClTx modified liposomes might be mediated by clathrin dependent and clathrin/caveolar/macropinocytosis independent pathways. Further, the endocytosis pathways were similar in the two cell types. The results were consistent with the previous report that the internalization of ClTx peptide in glioma cells was sensitive to chlorpromazine but not to filipin or amiloride [33].

3.5.2. Intracellular trafficking

The intracellular distributions of coumarin-6 (C6) loaded in ClTx conjugated liposomes in lysosomes and endoplasmic reticulum (ER) in two test cells are displayed qualitatively and quantitatively in Fig. 8 and Fig. 9, respectively. The Pearson's correlation (Pcc) was used here for the quantitative evaluation of co-localization between C6 and the organelles [34,35]. Firstly in U87 cells, compared to non-modified vehicles, the ClTx-modified liposomes showed more distribution in both organelles at 60 min and in ER at 20 min, without a significant difference in lysosomes at 20 min. This indicated that targeting liposomes were transported into the ER more quickly than the non-targeted group. Similarly, in A549 cells, the ClTx-modified liposomes accumulated more in both organelles at 60 min and in the ER at 20 min, without significant differences in lysosome at 20 min. These observations generally revealed that targeting liposomes enhanced the trafficking into both lysosomes and ER, and accelerated the transport into ER in comparison with non-modified ones. These characteristics of the intracellular trafficking of ClTx-modified liposomes in both cell lines were very similar. However, the distribution of C6 loaded in ClTx-conjugated

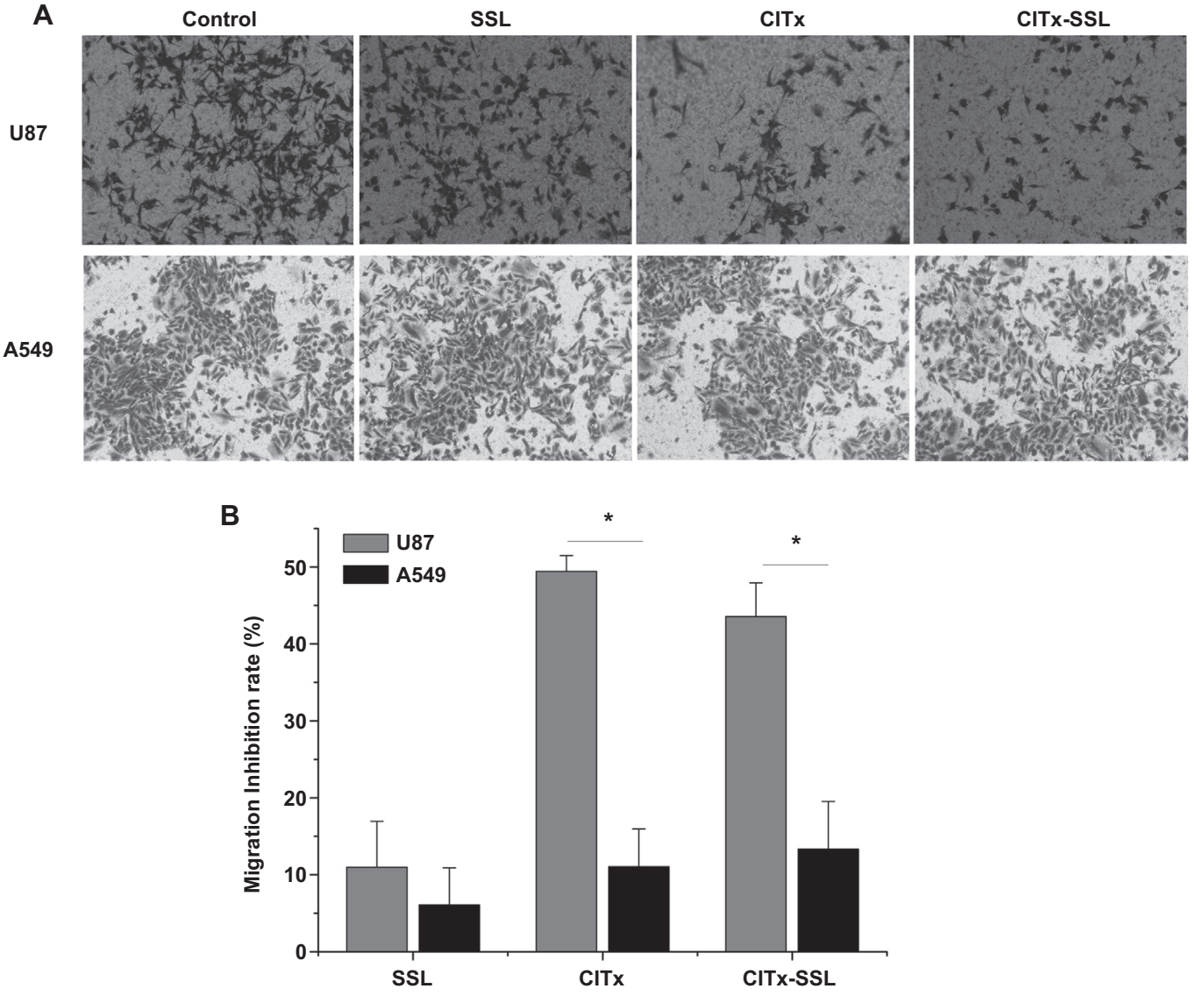

Fig. 11. Migration inhibition effect of ClTx, SSL and ClTx-SSL on U87 and A549 cells, and the cells treated with PBS as control group. A: Optical images of U87 and A549 cells on the bottom surface of the Transwell inserts after treatment with the ClTx, SSL and ClTx-SSL for 24 h. B: Quantitative assessment of the migration inhibition effect of ClTx, SSL and ClTx-SSL.

liposomes in two organelles was high in U87 cells but low in A549 cells, again consistent with the better uptake capacity of U87 cells confirmed by the study of cellular uptake (Fig. 4C). The high distribution of liposomes to lysosomes indicated that the clathrin mediated pathway was involved in the endocytosis of liposomes [36,37].

3.6. *In vivo targeting efficiency in a double tumor-bearing model*

With tumors grown on different sides of the subcutaneous dorsa in the same mouse, the double tumor-bearing model provided convenient and reliable comparability for the targeting efficiency of the same drug delivery system to two different tumors with minimum individual differences [38]. We found that the fluorescent signal of modified and non-modified liposomes in the A549 tumor was much stronger than that in the U87 tumor as shown in Fig. 10A. The difference might result from the dissimilar EPR effect based on different vascular permeability and density between different cell types [39–41]. In the same fluorescence intensity bar, the signal in the A549 tumor was too strong to observe the signal in U87 tumor, thus, the signals of the two tumors were imaged with different fluorescence intensity level as shown in Fig. 10B. ClTx-modified liposomes showed better targeting effect to both types of tumors than non-modified liposomes. The signal from DiR loaded in modified liposomes was higher in tumor site than that of non-modified liposomes from 6 h until 72 h, whereas this effect in U87 tumor only lasted from 6 h to 24 h. The *ex vivo* images of excised organs and tumors at 72 h as seen in Fig. 10C also demonstrated that ClTx modification increased the accumulation of liposomal DiR in A549 tumor. In U87 tumor, the signals of two liposomal formulations were similar at the end of test. In addition, high fluorescent signal was observed in liver and spleen, as expected due to the clearance of reticuloendothelial system (RES) [42]. In general, ClTx modification significantly increased the targeting effect of the two liposome systems whether in the U87 or A549 tumor.

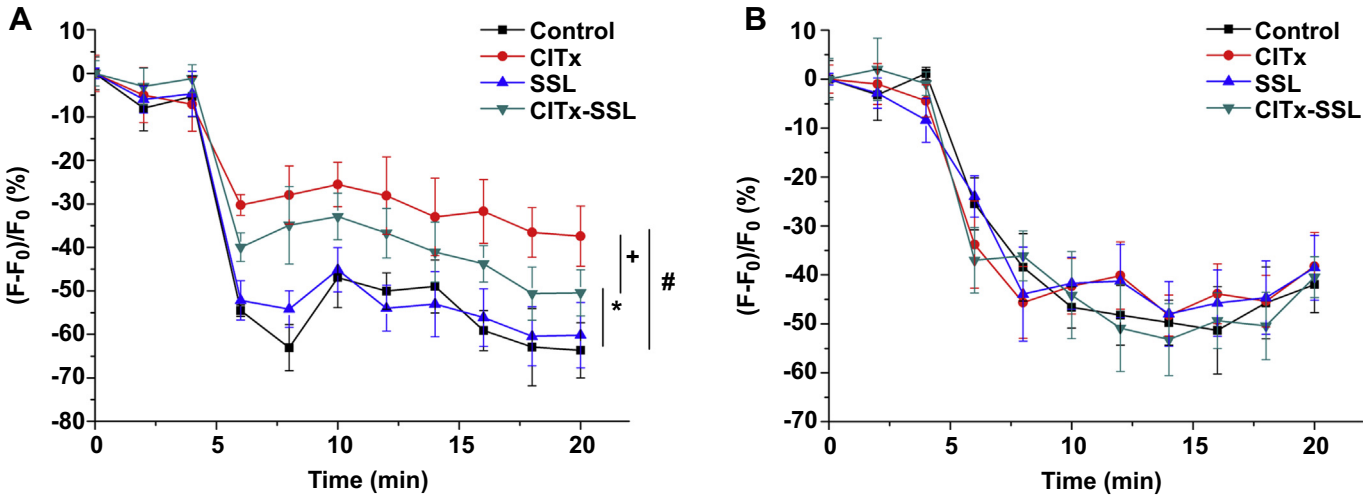

Fig. 12. Inhibition effect of ClTx, SSL and ClTx-SSL on ClC-3 by measurement of chloride current with MEQ on U87 (A) and A549 cells (B). F_0: the fluorescence intensity of dye at 0 min, F: the fluorescence intensity of dye at different time. The cells were incubated with isotonic solution without Cl^- at the first 6 min, and then the solution was replaced with hypotonic solution containing 30 mM Cl^-. (*, $p < 0.05$, significant difference between ClTx-SSL treated group and control group; #, $p < 0.05$, significant difference between ClTx treated group and control group; +, $p < 0.05$, significant difference between ClTx treated group and ClTx-SSL treated group).

Until now, ClTx-modified liposomes showed similar trends in these two tumor cells in terms of *in vitro* cell uptake, endocytosis pathway, intracellular trafficking and *in vivo* targeting efficacy, though U87 and A549 cells were very different in ClC-3 expression. This revealed that the targeted delivery of ClTx-modified liposomes to U87 tumor was actually mediated byMMP-2, therefore, this targeting system might also target to other cancers which express high level of MMP-2. Importantly, this study confirmed that the targeting delivery of ClTx-modified liposomes to the tumors was not relevant with the receptor-associated protein, chloride channel ClC-3.

Interestingly, it was found that the *in vitro* uptake of ClTx-conjugated liposomes in cells or in two organelles was higher in U87 cells but lower in A549 cells, whereas the *in vivo* accumulation of this targeted system was lower in U87 tumor but higher in A549 tumor. This finding indicated a poor correlation between *in vitro* and *in vivo* results, possibly due to biological differences between *in vitro* and *in vivo* models, including different interstitial fluid pressure, tumor microenvironment and so on, which need to be further studied [43–46].

3.7. The effect on ClC-3 of ClTx-modified liposomes

3.7.1. Migration assay

The transwell assay was used to compare the inhibitory effects of free ClTx, liposomes and ClTx modified liposomes on the migration of U87 and A549 cells, respectively. It can be clearly seen in the Fig. 11 that the free ClTx and ClTx-modified liposomes inhibited the migration of U87 cells compared to the control group, whereas the non-modified liposomes did not produce such an inhibitory effect. Interestingly, the free ClTx, modified liposomes as well as non-modified ones did not limit the migration of A549 cells. It is known that ClC-3 is a type of chloride channel that regulates the volume of cells. When the cells migrate through the 8 μm pores in the transwell, the cells have to shrink by releasing Cl^- and K^+ through various ion channels including ClC-3, and driving the water efflux through water channel or aquaporins [15]. The study mentioned above confirmed that the receptor for ClTx was MMP-2, and that MMP-2 co-localized with ClC-3 in cellular membrane domain as a protein complex. Therefore, the inhibitory effect on cell migration by ClTx and modified liposomes was probably because the protein complex was internalized into the cells, resulting in decreased level of ClC-3 on the surface of cells when ClTx binds to MMP-2, and as a result, the cell migration was limited. The differences in the migration inhibition by ClTx and modified liposomes between the two cell lines were most likely due to the different level of ClC-3 on the cell surface. In the cancer therapy, this modified drug delivery system may inhibit tumor metastasis based on the traditional targeting therapeutic effect because migration is a necessary step in tumor metastasis [47].

3.7.2. Measurement of chloride currents by MEQ

To further determine the effect of ClTx, SSL and ClTx-SSL on the ClC-3, MEQ, a chloride-sensitive dye was used to measure the chloride fluxes. When cell-permeable DiH-MEQ moved across the cellular membrane, it was oxidized to the positively charged and chloride sensitive MEQ by intracellular oxidation. Fig. 12A shows that the addition of a hypotonic solution with 30 mM Cl^- triggered the quenching of MEQ fluorescence in the U87 cells sharply in the control and SSL groups. The U87 cells pretreated with ClTx or ClTx-SSL showed less cell permeability for Cl^-, indicating that ClTx, whether free or modified on liposomes, had inhibitory effect on chloride channels, probably ClC-3. Specifically, compared with the control group, the free ClTx reduced the Cl^- currents by 40%, and the ClTx-SSL reduced the currents by 20%. The difference in the Cl^- current inhibition effect between ClTx and ClTx-SSL was probably because the free ClTx bound the receptor more quickly and easily than ClTx-modified liposomes. As expected, SSL did not show a significant inhibitory effect on the Cl^- currents. However, in the case of A549 cells shown in Fig. 12B, ClTx, SSL or ClTx-SSL did not affect the chloride current compared to the control group. This indicated that the ClTx and ClTx-SSL had effect only on U87 cells, consistent with the data from the migration assay, likely due to the different expression levels of ClC-3 between the two cell lines.

Generally, it was demonstrated that ClTx modification on the liposomes affected the receptor-related protein ClC-3 via binding with receptor MMP-2, leading to the inhibition of cell migration and chloride currents through the internalization of the protein complex containing MMP-2 and ClC-3 probably [16,48,49]. This is also highly significant because cell migration is a key step in tumor metastasis.

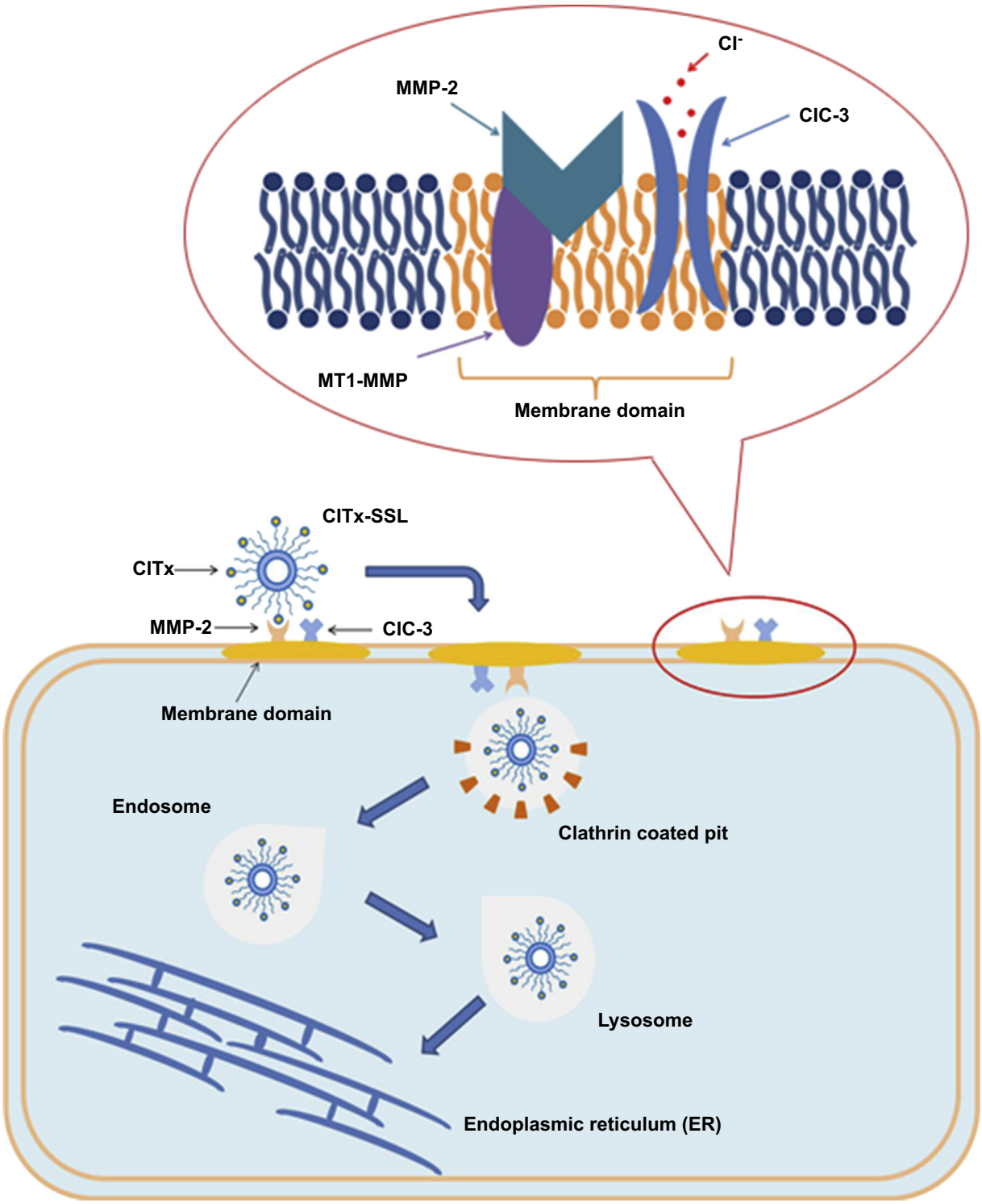

Fig. 13. Schematic diagram of the ClTx modified liposomes targeting to MMP-2 and its effect on the ClC-3 located in membrane domain with MMP-2 in U87 cells, including the intracellular trafficking of ClTx-SSL.

4. Conclusions

In summary, ClTx modification enhances the *in vitro* and *in vivo* targeting ability of liposomes in both types of U87 and A549 cells via MMP-2 mediation but independent of ClC-3. The endocytosis pathways of the liposomes in both types of cells are clathrin dependent and the ClTx modification increases the transport of liposomes to lysosomes and ER in both cell types. Further, in the U87 cells, the ClTx modification affects the ClC-3, a receptor-associated protein located close to MMP-2. The schematic diagram shown in Fig. 13 illustrates this process. In particular, when the ClTx attached to the surface of liposomes interacts with the MMP-2 on the cells, the liposomes enter the cell through MMP-2 mediation. At the same time, the protein complex containing

MMP-2 and ClC-3 is internalized, the chloride currents are blocked indirectly and the cell migration is inhibited. This drug delivery system with ClTx modification may enhance the targeting to tumors with high level of MMP-2 and induce the inhibitory effect on tumor metastasis, because ClC-3 is a key factor in cell migration, which is a necessary step in tumor metastasis.

Acknowledgments

This work was supported by the National Natural Science Foundation of China (81130059), the National Research Fund for Fundamental Key Project (2009CB930300) and the Innovation Team of Ministry of Education (No. BMU20110263), National Basic Research Program of China (973 program, 2013CB932501).

References

[1] Stevens TJ, Arkin IT. Do more complex organisms have a greater proportion of membrane proteins in their genomes? Proteins 2000;39:417–20.
[2] Wallin E, von Heijne G. Genome-wide analysis of integral membrane proteins from eubacterial, archaean, and eukaryotic organisms. Protein Sci 1998;7:1029–38.
[3] Schey KL, Grey AC, Nicklay JJ. Mass spectrometry of membrane proteins: a focus on aquaporins. Biochemistry 2013;52:3807–17.
[4] Wu CC, Yates 3rd JR. The application of mass spectrometry to membrane proteomics. Nat Biotechnol 2003;21:262–7.
[5] Haley B, Frenkel E. Nanoparticles for drug delivery in cancer treatment. Urol Oncol 2008;26:57–64.
[6] Byrne JD, Betancourt T, Brannon-Peppas L. Active targeting schemes for nanoparticle systems in cancer therapeutics. Adv Drug Deliv Rev 2008;60:1615–26.
[7] Arayne MS, Sultana N. Review: nanoparticles in drug delivery for the treatment of cancer. Pak J Pharm Sci 2006;19:258–68.
[8] Hrkach J, Von Hoff D, Mukkaram Ali M, Andrianova E, Auer J, Campbell T, et al. Preclinical development and clinical translation of a PSMA-targeted docetaxel nanoparticle with a differentiated pharmacological profile. Sci Transl Med 2012;4:128ra39.
[9] DeBin JA, Maggio JE, Strichartz GR. Purification and characterization of chlorotoxin, a chloride channel ligand from the venom of the scorpion. Am J Physiol 1993;264:C361–9.
[10] Deshane J, Garner CC, Sontheimer H. Chlorotoxin inhibits glioma cell invasion via matrix metalloproteinase-2. J Biol Chem 2003;278:4135–44.
[11] Olsen ML, Schade S, Lyons SA, Amaral MD, Sontheimer H. Expression of voltage-gated chloride channels in human glioma cells. J Neurosci 2003;23:5572–82.
[12] Ullrich N, Gillespie GY, Sontheimer H. Human astrocytoma cells express a unique chloride current. NeuroReport 1996;7:1020–4.
[13] Ullrich N, Bordey A, Gillespie GY, Sontheimer H. Expression of voltage-activated chloride currents in acute slices of human gliomas. Neuroscience 1998;83:1161–73.
[14] Jentsch TJ. CLC chloride channels and transporters: from genes to protein structure, pathology and physiology. Crit Rev Biochem Mol Biol 2008;43:3–36.
[15] Stauber T, Weinert S, Jentsch TJ. Cell biology and physiology of CLC chloride channels and transporters. Compr Physiol 2012;2:1701–44.
[16] McFerrin MB, Sontheimer H. A role for ion channels in glioma cell invasion. Neuron Glia Biol 2006;2:39–49.
[17] Shen S, Khazaeli MB, Gillespie GY, Alvarez VL. Radiation dosimetry of 131I-chlorotoxin for targeted radiotherapy in glioma-bearing mice. J Neurooncol 2005;71:113–9.
[18] Veiseh M, Gabikian P, Bahrami SB, Veiseh O, Zhang M, Hackman RC, et al. Tumor paint: a chlorotoxin:Cy5.5 bioconjugate for intraoperative visualization of cancer foci. Cancer Res 2007;67:6882–8.
[19] Kievit FM, Veiseh O, Fang C, Bhattarai N, Lee D, Ellenbogen RG, et al. Chlorotoxin labeled magnetic nanovectors for targeted gene delivery to glioma. ACS nano 2010;4:4587–94.
[20] Huang R, Ke W, Han L, Li J, Liu S, Jiang C. Targeted delivery of chlorotoxin-modified DNA-loaded nanoparticles to glioma via intravenous administration. Biomaterials 2011;32:2399–406.
[21] Xiang Y, Liang L, Wang X, Wang J, Zhang X, Zhang Q. Chloride channel-mediated brain glioma targeting of chlorotoxin-modified doxorubicine-loaded liposomes. J Control Release 2011;152:402–10.
[22] Vichai V, Kirtikara K. Sulforhodamine B colorimetric assay for cytotoxicity screening. Nat Protoc 2006;1:1112–6.
[23] Kessenbrock K, Plaks V, Werb Z. Matrix metalloproteinases: regulators of the tumor microenvironment. Cell 2010;141:52–67.
[24] Bauvois B. New facets of matrix metalloproteinases MMP-2 and MMP-9 as cell surface transducers: outside-in signaling and relationship to tumor progression. Biochim Biophys Acta 2012;1825:29–36.
[25] Zhao Z, Li X, Hao J, Winston JH, Weinman SA. The ClC-3 chloride transport protein traffics through the plasma membrane via interaction of an N-terminal dileucine cluster with clathrin. J Biol Chem 2007;282:29022–31.
[26] Sahay G, Alakhova DY, Kabanov AV. Endocytosis of nanomedicines. J Control Release 2010;145:182–95.
[27] Treuel L, Jiang X, Nienhaus GU. New views on cellular uptake and trafficking of manufactured nanoparticles. J R Soc Interface 2013;10:20120939.
[28] Yao D, Ehrlich M, Henis YI, Leof EB. Transforming growth factor-beta receptors interact with AP2 by direct binding to beta2 subunit. Mol Biol Cell 2002;13:4001–12.
[29] Damke H, Baba T, van der Bliek AM, Schmid SL. Clathrin-independent pinocytosis is induced in cells overexpressing a temperature-sensitive mutant of dynamin. J Cell Biol 1995;131:69–80.
[30] Smart EJ, Anderson RG. Alterations in membrane cholesterol that affect structure and function of caveolae. Methods Enzymol 2002;353:131–9.
[31] Kerr MC, Teasdale RD. Defining macropinocytosis. Traffic 2009;10:364–71.
[32] Ziello JE, Huang Y, Jovin IS. Cellular endocytosis and gene delivery. Mol Med 2010;16:222–9.
[33] Wiranowska M, Colina LO, Johnson JO. Clathrin-mediated entry and cellular localization of chlorotoxin in human glioma. Cancer Cell Int 2011;11:27.
[34] Zinchuk V, Zinchuk O, Okada T. Quantitative colocalization analysis of multicolor confocal immunofluorescence microscopy images: pushing pixels to explore biological phenomena. Acta Histochem Cytochem 2007;40:101–11.
[35] Zinchuk V, Grossenbacher-Zinchuk O. Recent advances in quantitative colocalization analysis: focus on neuroscience. Prog Histochem Cytochem 2009;44:125–72.
[36] Khalil IA, Kogure K, Akita H, Harashima H. Uptake pathways and subsequent intracellular trafficking in nonviral gene delivery. Pharmacol Rev 2006;58:32–45.
[37] Pryor PR, Luzio JP. Delivery of endocytosed membrane proteins to the lysosome. Biochim Biophys Acta 2009;1793:615–24.
[38] Wang Z, Yu Y, Dai W, Lu J, Cui J, Wu H, et al. The use of a tumor metastasis targeting peptide to deliver doxorubicin-containing liposomes to highly metastatic cancer. Biomaterials 2012;33:8451–60.
[39] Maeda H, Nakamura H, Fang J. The EPR effect for macromolecular drug delivery to solid tumors: improvement of tumor uptake, lowering of systemic toxicity, and distinct tumor imaging in vivo. Adv Drug Deliv Rev 2013;65:71–9.
[40] Prabhakar U, Maeda H, Jain RK, Sevick-Muraca EM, Zamboni W, Farokhzad OC, et al. Challenges and key considerations of the enhanced permeability and retention effect for nanomedicine drug delivery in oncology. Cancer Res 2013;73:2412–7.
[41] Torchilin V. Tumor delivery of macromolecular drugs based on the EPR effect. Adv Drug Deliv Rev 2011;63:131–5.
[42] Storm G, Belliot SO, Daemen T, Lasic DD. Surface modification of nanoparticles to oppose uptake by the mononuclear phagocyte system. Adv Drug Deliv Rev 1995;17:31–48.
[43] Heldin CH, Rubin K, Pietras K, Ostman A. High interstitial fluid pressure – an obstacle in cancer therapy. Nat Rev Cancer 2004;4:806–13.
[44] Jain RK. Normalizing tumor microenvironment to treat cancer: bench to bedside to biomarkers. J Clin Oncol 2013;31:2205–18.
[45] Duncan R, Sat-Klopsch YN, Burger AM, Bibby MC, Fiebig HH, Sausville EA. Validation of tumour models for use in anticancer nanomedicine evaluation: the EPR effect and cathepsin B-mediated drug release rate. Cancer Chemother Pharmacol 2013;72:417–27.
[46] Griffon-Etienne G, Boucher Y, Brekken C, Suit HD, Jain RK. Taxane-induced apoptosis decompresses blood vessels and lowers interstitial fluid pressure in solid tumors: clinical implications. Cancer Res 1999;59:3776–82.
[47] Chambers AF, Groom AC, MacDonald IC. Dissemination and growth of cancer cells in metastatic sites. Nat Rev Cancer 2002;2:563–72.
[48] Polette M, Birembaut P. Membrane-type metalloproteinases in tumor invasion. Int J Biochem Cell Biol 1998;30:1195–202.
[49] Kasai T, Nakamura K, Vaidyanath A, Chen L, Sekhar S, El-Ghlban S, et al. Chlorotoxin fused to IgG-Fc inhibits glioblastoma cell motility via receptor-mediated endocytosis. J Drug Deliv 2012;2012:975763.